ELSEVIER

Catalysis Today 33 (1997) 57–71

CATALYSIS TODAY

The partial oxidation of C_5 hydrocarbons over vanadia-based catalysts

Umit S. Ozkan *, Todd A. Harris, Brian T. Schilf

Department of Chemical Engineering, The Ohio State University, Columbus, Ohio 43210, USA

Abstract

The partial oxidation of C_5 hydrocarbons was investigated over unpromoted and alkali-promoted V_2O_5 catalysts. Products of this mild oxidation reaction include both maleic and phthalic anhydride. The apparent effect of alkali promotion is to facilitate the loss of surface oxygen species which are important in the activation of alkanes and the complete oxidation of intermediate species. Studies performed using 1-pentene as feed have indicated that once the first oxidative dehydrogenation step is eliminated, pentene oxidation proceeds readily towards maleic and phthalic anhydride formation. The use of 1-pentene in the feed stream caused a bulk reduction of the catalyst from V_2O_5 to VO_2 in the presence of gas phase oxygen.

1. Introduction

There is growing interest in the partial oxidation of the C_5 fraction of the hydrocarbon stream from naphtha steam crackers as a result of several factors. The C_5 stream consists of mostly n-pentane and cyclopentane, neither of which have found a market in which they can be sold, and they are currently being used as fillers in gasoline. Recent legislation, however, has limited the Reid vapor pressure which will limit the amount of C_5 alkanes that can be added to gasoline, further increasing their availability. The possibility of transforming these low value hydrocarbon fractions into a high value product remains as a good incentive for research. Furthermore, the activation and partial oxidation of lower alkanes continues to pose a challenge for catalysis researchers. Especially, in the case of pentane oxidation to form phthalic anhydride, the challenge is even greater since the catalyst needs not only to activate the alkane molecule, but also promote the formation of C–C bonds in an oxidative medium.

Currently, there are several important industrial processes which transform low value hydrocarbons into valuable industrial products. For example, n-butane is transformed into maleic anhydride over a vanadium–phosphorous–oxide (VPO) catalyst, and *ortho*-xylene is transformed into phthalic anhydride over a vanadium oxide catalyst. These two processes are related to C_5 partial oxidation because the two products, maleic anhydride and phthalic anhydride, can both be produced from the partial oxidation of n-pentane.

The first known study of C_5 partial oxidation was a survey of the behavior of 1-pentene and

* Corresponding author. Tel.: +1-614-2926623; fax: +1-614-2923769; e-mail: ozkan.1@osu.edu.

PII S0920-5861(96)00136-8

several branched-chain pentenes over V_2O_5 [1–3]. Butt and Fish determined that the mechanism of alkene adsorption consists of the donation of a π electron to a surface V^{5+} site and a corresponding isomerization of 1-pentene to 2-pentene. The 2-pentene then goes on to react with surface oxygen, reducing the catalyst, and desorbs as a partially oxygenated species. The catalyst is then reoxidized by gas phase oxygen to the original oxidation state. Included in the products of the partial oxidation of 1-pentene was maleic anhydride.

There have been several vanadia-based catalysts tested for the partial oxidation of n-pentane. The oxidation of n-pentane over 12-molybdo-vanadophosphoric acid was found to produce only maleic anhydride and complete oxidation products, CO and CO_2. However, as the reaction was allowed to continue, the catalyst underwent a surface reduction which increased the rate of decomposition of the crystal structure, thus deactivating the catalyst [4].

When V_2O_5 supported on SiO_2 was used for n-pentane partial oxidation, the major products were reported to be CO, CO_2, 1-pentene, 2-pentene, and maleic anhydride. The authors suggested that a highly dispersed phase of vanadia promoted the dehydrogenation reactions and isolated crystalline V_2O_5 sites promoted oxygen insertion and combustion reactions [5]. When V_2O_5 was combined with P_2O_5, forming $(VO)_2P_2O_4$, the products of the reaction with n-pentane in the presence of oxygen included not only complete oxidation products, but also maleic and phthalic anhydrides. When V_2O_5 is combined with MoO_3 the partial oxidation of n-pentane yielded CO_x and maleic anhydride in smaller yields than when P_2O_5 was used. When TiO_2 was used as the support, no anhydride products were seen [6].

While the VPO catalysts remain as the most commonly studied materials for n-pentane oxidation as evidenced by the reports that appeared in the literature [7–15], the formation of the two anhydrides on VPO surfaces involves a series of complex reactions that are not completely understood. It appears that 1,3-pentadiene is a common intermediate in the formation of both of the anhydrides, with maleic anhydride forming through furan as an intermediate. Phthalic anhydride formation, on the other hand is suggested to take place through a ring closure step with a corresponding loss of allylic hydrogens, to form cyclopentadiene and a surface template addition reaction between two cyclopentadiene molecules followed by oxygen insertion to form phthalic anhydride [9].

In this study, unsupported V_2O_5 and alkali-promoted V_2O_5 catalysts were used in pentane and pentene oxidation. Reaction studies were performed with two different n-pentane/oxygen ratios and with 1-pentene in place of n-pentane. Characterization studies included BET surface area measurement, X-ray diffraction, Raman spectroscopy, X-ray photoelectron spectroscopy, temperature programmed reduction and desorption. The objectives of this study were to determine the activity of unsupported V_2O_5, the effect of alkali promotion on the product distribution, and the effect of bypassing the first oxidative dehydrogenation of n-pentane.

2. Experimental

2.1. Catalyst preparation and characterization

Crystalline V_2O_5 was prepared by the decomposition of ammonium metavanadate (NH_4VO_3 from Aldrich, C.A.S. [7803-55-6]) with oxygen increasing the temperature from room temperature to 500°C at 2°C/min and continuing the process at 500°C for an additional 4 h. The reaction was carried out in a temperature programmable Lindberg furnace type 59544-ES. The resulting V_2O_5 crystals, which were orange–brown in color and rectangular in shape, were then placed in double distilled water in a round bottom flask equipped with a Teflon stirrer and allowed to stir for 5 h. After water treatment the resulting slurry was dried in a Büchi model RE121 rotovapor apparatus with a

bath temperature of 70°C. After drying, the catalyst was removed from the flask and again calcined with oxygen at 500°C for 4 h. The purpose of the water treatment was to give the unpromoted V_2O_5 the same history as the promoted V_2O_5, as will be discussed in the following section.

V_2O_5 was promoted with Na, Li, and K in the form of carbonates from Baker and with the following C.A.S. numbers, respectively: [3607-01], [2362-1], and [3012-5]. The promoted V_2O_5 was synthesized using the procedure described in the previous section except for the water treatment step. After the V_2O_5 was added to water, it was allowed to stir for 1 h and then the desired amount of alkali carbonate to provide an alkali metal to V_2O_5 molar ratio of 1:100 was dissolved in the slurry and the mixture was allowed to stir for an additional 4 h. Rotovapor drying and final calcination followed. After final calcination, all four samples were in the form of a fine powder which was then sifted through an 80 mesh sieve to assure uniform particle size.

The catalysts were characterized by krypton BET surface area measurement, X-ray diffraction, Raman spectroscopy, X-ray photoelectron spectroscopy, temperature programmed reduction (TPR), and temperature programmed desorption (TPD).

BET surface area measurement was done using a Micromeritics AccuSorb 2100E instrument with krypton as the adsorbate. X-ray diffraction patterns were obtained using a Scintag PAD-V Diffractometer with Cu Kα radiation ($\lambda = 1.5432$ Å) as the source. A SPEX Triplemate Raman spectrometer which used a 5-W Argon ion laser (Spectra Physics, model 2017) was used to obtain Raman spectra. The spectrometer was equipped with both PMT and CCD detectors. X-ray photoelectron spectroscopy was done on a Fissons Instruments, model ESCA Lab Mark II using Mg Kα radiation (1253.6 eV). Binding energies were referenced to C 1s line of 284.6 eV. The temperature programmed desorption and reduction experiments were done on a system built in-house and has been described previously [16]. TPR profiles were obtained by heating samples (100 mg) at a rate of 5°C/min to 900°C and holding them at this temperature for 10 min. The reducing gas consisted of 6% H_2 in N_2 at a flow of 60 sccm. In TPD experiments, the catalysts were calcined in-situ prior to any adsorption followed by a vacuum treatment at 200°C for 2 h. The adsorbates, pentane and pentene (5%), were passed over the catalyst at room temperature for 2 h at a flow rate of 30 cm^3(STP)/min. After flushing the catalyst for 1 h with helium, the temperature program was started, with a heating rate of 15°C/min up to 600°C, followed by an isothermal step at 600°C for 20 min. The species desorbing from the surface were analyzed by a mass spectrometer.

2.2. Reaction experiments

The partial oxidation of n-pentane over alkali promoted V_2O_5 was carried out in a tubular fixed bed reactor. All tubing except the condenser tube was 1/4 in. 304 stainless steel and the condenser tube was 14 in. Vicore© from Corning. The reactor system consisted of four parts: feed, reactor, condenser, and analytical.

The feed system consisted of three high pressure gas cylinders, each with a mass flow controller. The feed gases were 5.0% n-pentane in high purity nitrogen (specialty mixture from Matheson), oxygen (extra dry grade from Gas Techniques), and nitrogen (from Liquid Carbonic). The mass flow controllers were Brooks model 5850E and the controller box was Brooks model 5878. The gases were metered to the proper flow and then allowed to mix in a 1/2 in. diameter stainless steel manifold filled with silica gel beads to aid in mixing and remove any water present. The reactants were then sent on to the reactor.

The reactor consisted of a 1/4 in. diameter by 11 in. long stainless steel, id = 4.8 mm, or quartz, id = 4.0 mm, 'u-tube' immersed in a heated, fluidized sand bath (Techne model FB-

08 fluidized bath). The reactor itself was packed with the catalyst bed in the exit arm of the tube. The catalyst bed was held in place by 2 cm long plugs of quartz wool and the rest of the reactor tube was filled with inert ceramic beads (ER120A size 1.6–2.5 mm ceramic beads from SEPR, Mountainside, NJ) to aid in mixing, assure proper heat transfer, and quench gas phase cracking reactions. The reactor was connected to the rest of the system by Cajon© quick connect vacuum fittings. The outlet arm between the reactor and the condenser was wrapped with heating tape and kept at a temperature of approximately 300°C.

The condenser consisted of a 1/4 in. diameter by 12 in. long 'u-tube' made from Vicore©, Corning. The condenser was attached to the system using Cajon© quick connect vacuum fittings and was kept at room temperature. The purpose of the condenser was to catch any large organic products, which could be dissolved in acetonitrile for HPLC analysis.

The analytical system consisted of two parts, gas chromatography (GC) and high performance liquid chromatography (HPLC). GC was used to analyze the reaction products that were in gas phase at room temperature and HPLC was used to analyze reaction products that were solid at room temperature.

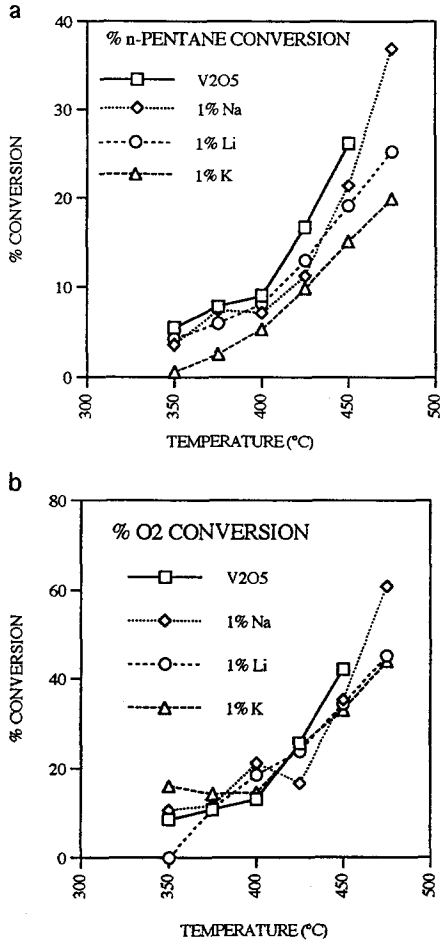

Fig. 1. % Conversion of n-pentane and oxygen as a function of temperature in n-pentane oxidation (2.5% n-pentane, 10% O_2).

Table 1
X-ray diffraction data

Sample	d (Å)	[hkl]	I/I_0	$I_{[101]}/I_{[010]}$
V_2O_5	4.11	101	100	1.0
	3.20	010	100	
	2.70	400	64	
	5.38	301	39	
1%Li/V_2O_5	4.11	101	100	1.34
	3.20	010	75	
	2.70	400	55	
	5.38	301	24	
1%Na/V_2O_5	4.11	101	100	1.21
	3.20	010	83	
	2.70	400	60	
	5.38	301	26	
1%K/V_2O_5	4.11	101	100	1.27
	3.20	010	79	
	2.70	400	68	
	5.38	301	26	

The on-line gas chromatograph (Hewlett–Packard, 5890A) was equipped with a thermal conductivity detector (TCD) and a flame ionization detector (FID). Sample injection was accomplished using two six-port valves and column isolation for permanent gas analysis was accomplished with a four-port valve. Gas separation for the FID was accomplished by the use of a 25 foot, 1/8 in., stainless steel column packed with Chromosorb P AW, 23% SP-1700, 80/100 mesh packing from Supelco. This column was operated isothermally at 140°F. Separation for TCD was accomplished with the use

of two columns. A molecular sieve 5A, 60/80 Mesh from Supelco and a HayeSep D, 100/120 mesh from Supelco. Two Hewlett–Packard integrators (Models 3390A and 3396A) were used to process the signals from the detectors.

The HPLC system used in this work consisted of a Spectra-Physics model SCM400 Degasser, a SpectraSYSTEM model P4000 gradient pump, a SpectraSYSTEM model MUV2000 detector, and a Spectra-Physics SP4270 integrator. The column used was a Spherisorb 5 ODS-2 250 mm × 4.6 mm C-18 reverse phase column from Chromopack. A sample size of 20 μl was used. During a chromatographic analysis the pump was run in a gradient mode with the following linear solvent program and at a flow rate of 1 ml/min. At the beginning of the analysis the solvent consisted of 50% acetonitrile and 50% water and at the end of 5 min the solvent consisted of 60/40 acetonitrile/water. HPLC analysis was performed off-line to take advantage of the higher sensitivity of this technique.

Studies with n-pentane were conducted using 0.7 m^2 of catalyst, a bed length of 4.5 cm, a retention time of 0.63 s, and a total flow of 39.2 cm^3/min. The feed composition was 2.5% n-pentane, 10% oxygen, and the balance nitrogen. A stainless steel reactor was used for these studies.

To determine the effect of the ratio of oxygen to n-pentane in the feed, studies were done with a feed composition of 1.2% n-pentane, 10% oxygen, and the balance nitrogen. The retention time was reduced to 0.43 s for this set of experiments. The reactor used for these studies was a quartz reactor of the same design as used in the previously described studies.

Studies were done with 1-pentene feed replacing n-pentane to determine the yield and product distribution when the first oxidative dehydrogenation step of n-pentane is eliminated. 1-pentene studies were conducted with the feed composition of 1.5% 1-pentene, 10% oxygen, and the balance nitrogen. The catalyst bed length was 2 cm, the total surface area was 0.1 m^2, the retention time was 0.28 s, and the total flow was 27 cm^3/min.

3. Results

3.1. Catalyst characterization

The surface area of unpromoted V_2O_5 was 4.8 m^2/g. The effect of the alkali promotion was to decrease the specific surface area to 4.1, 4.2, and 2.1 m^2/g for Li-, Na-, and K-promoted catalysts, respectively. Each of the surface area measurements was repeated at least twice. The error in surface area measurements using krypton as the adsorbate was less then 0.1 m^2/g.

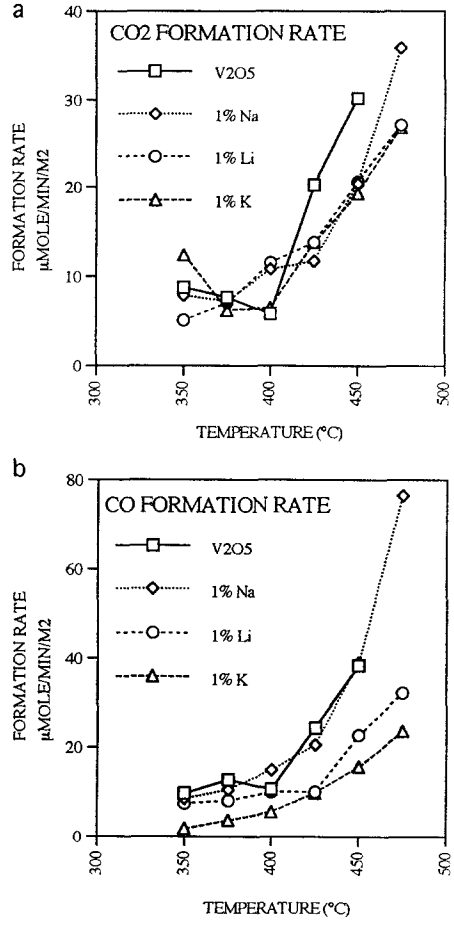

Fig. 2. Observed formation rates of CO and CO_2 in n-pentane oxidation (2.5% n-pentane, 10% O_2).

X-ray diffraction data and Raman spectroscopy data confirmed that the samples remained as V_2O_5, but did not show any significant differences between the promoted and unpromoted catalyst. Table 1 shows the *d*-spacing values and the corresponding relative intensities for the four catalysts. One major difference was in the intensity ratios of [101] to [010] reflections where the promoted catalysts showed a reduction in the intensity of the reflections resulting from the basal plane. There was no discernible differences in the line widths that could have suggested a difference in particle size. X-ray photoelectron spectroscopy showed that the vanadium was in the 5 + oxidation state in both the promoted and the unpromoted samples, also that the alkalis were present in the 1 + oxidation state. The alkali metals were seen to be concentrated primarily on the surface, giving alkali metal to vanadium atomic ratios of about 0.1 as opposed to a ratio of 0.005 that one would expect if the alkali metal were distributed uniformly in the bulk. Temperature programmed reduction (TPR) yielded five reduction peaks and demonstrated little difference between the promoted and unpromoted catalysts.

3.2. Oxidation studies

Blank reactor studies were conducted at the identical conditions which were used for reac-

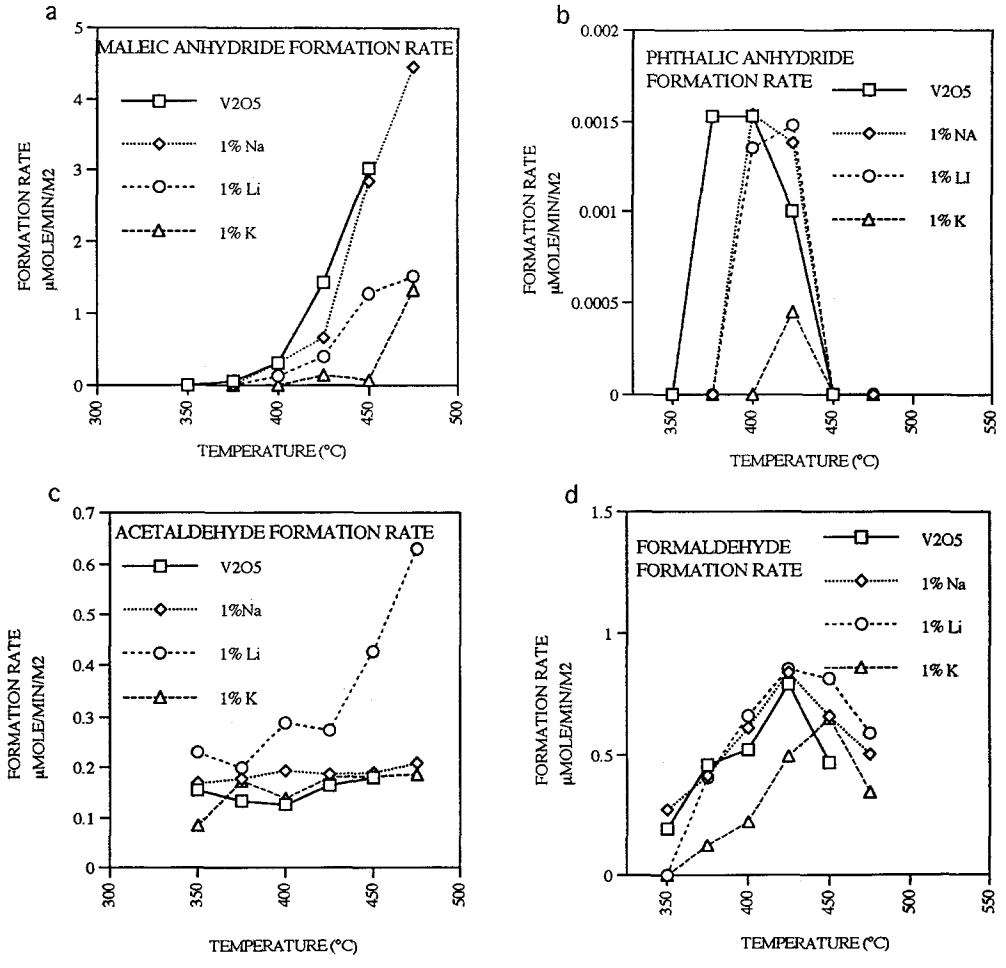

Fig. 3. Observed formation rates of partial oxidation products in n-pentane oxidation (2.5% n-pentane, 10% O_2).

tion studies. Blank reaction studies done with the stainless steel reactor showed that there was some conversion, especially at the highest temperatures studied, with the only products formed being carbon oxides. Blank studies done using a quartz reactor yielded negligible conversion at all temperatures studied.

Oxidation experiments with a feed mixture of 2.5% n-pentane, 10% oxygen, and the balance nitrogen gave reaction products of CO_2, CO, H_2O, maleic anhydride, phthalic anhydride, 2-methyl-3,5-furandione, and at the higher temperatures trace amounts of cracking products like ethylene, propylene. The reaction data were obtained after steady-state was reached, which typically took 4–6 h for pentane oxidation experiments. The transient period before reaching steady-state was much longer (24–48 h) for pentene oxidation experiments. After reaching steady-state, the catalyst was kept on line for a minimum of 8 h. During this time period, no aging effects were observed over the catalyst. It should also be noted that the conversion data presented here were not normalized in a mathematical sense, however, the surface area used was kept constant, thereby inherently normalizing the data.

Fig. 1a shows a plot of C_5 conversion as a function of temperature for all four of the catalysts studied. In all cases the conversion in-

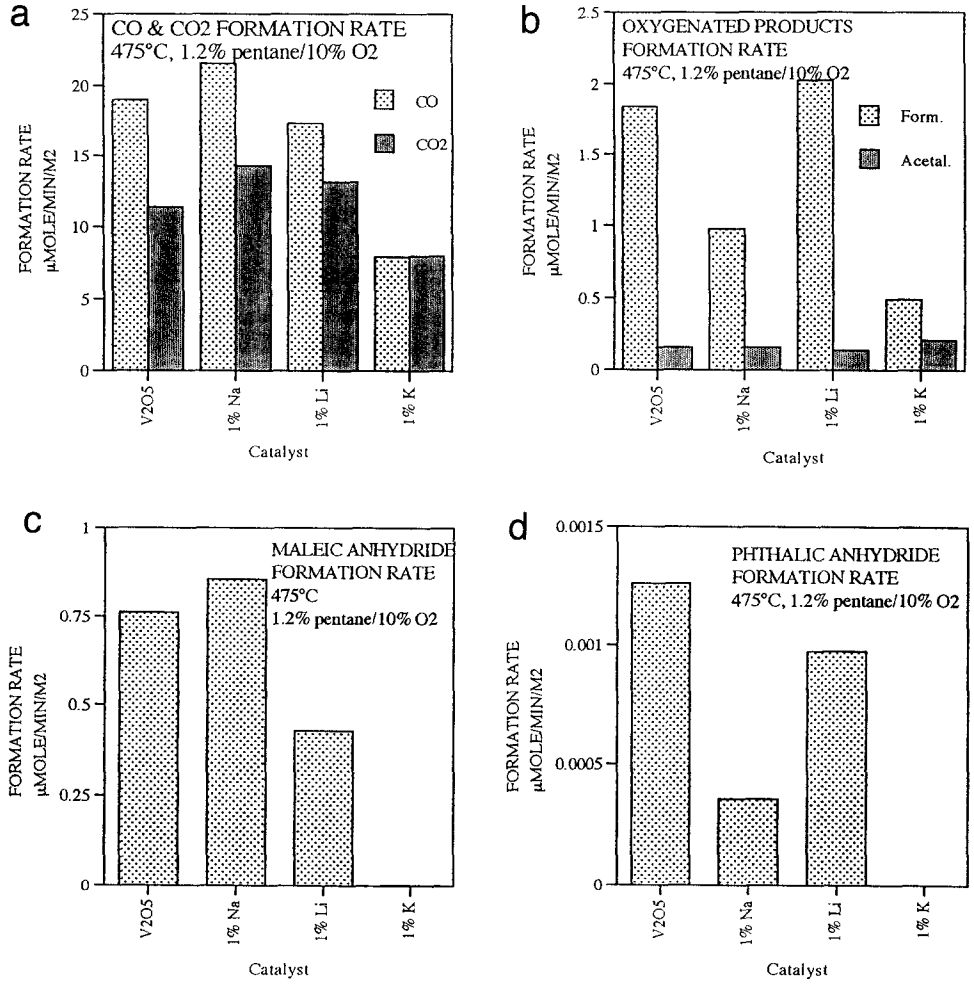

Fig. 4. Observed formation rates in n-pentane oxidation (1.2% n-pentane, 10% O_2).

creases with temperature and the activity is highest over the unpromoted V_2O_5 and lowest over the K-promoted catalysts. A plot of O_2 conversion versus temperature is presented in Fig. 1b and demonstrates a similar trend as seen for C_5 conversion, that it increases with increasing temperature. The data point at 475°C has been left out for unpromoted V_2O_5 since this set of conditions led to complete conversion of oxygen and severe reduction of the catalyst. CO and CO_2 formation rates (μmol/min/m^2) also tended to increase with increasing temperature, but were generally lower over the alkali promoted catalysts (Fig. 2). The observed formation rates of partial oxidation products are presented in Fig. 3. In all cases, the formation rate of maleic anhydride is nearly negligible until a reaction temperature above 400°C is used. Also in all cases, the formation rate of maleic anhydride (Fig. 3a) was greater over the unpromoted V_2O_5. Formation rate of phthalic anhydride, shown in Fig. 3b, reached a maximum value between 375 and 425°C and then decreased to zero by 450°C. The maximum formation rate of phthalic anhydride was moved to higher temperatures in the presence of the alkali promoters. The formation rate of partially oxygenated products like formaldehyde and acetaldehyde were, in general, greater in the presence of the alkali promoters, except in the case of the K promoter, over which the overall conversion was very low (Fig. 3c and d). It is interesting to note that the formation rate of formaldehyde, similar to phthalic anhydride, went through a maximum as reaction temperature was increased.

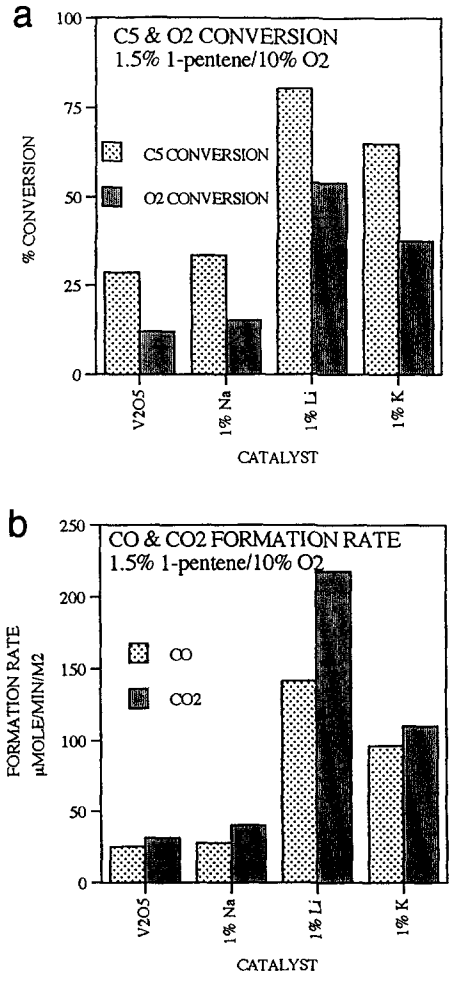

Fig. 5. 1-Pentene oxidation (1.5% 1-pentene, 10% O_2) (a) % conversion of 1-pentene and O_2. (b) Formation rates of carbon oxides.

Reactions experiments were also performed at increased oxygen to pentane ratios using a pentane concentration of 1.2% and an oxygen concentration of 10%. Results obtained at 475°C are presented in Fig. 4. One notable feature in these results was that the K-promoted catalyst had the lowest conversion level (around 15% as opposed to 25% for the unpromoted catalyst) and the phthalic and maleic anhydride yields over this catalyst were essentially zero while the unpromoted V_2O_5 performed better in both accounts.

When 1-pentene was used as feed in place of n-pentane, the activity of the catalysts was much higher reaching complete conversion very rapidly. The results presented were obtained using a lower retention time of 0.28 s and a reaction temperature of 375°C. Fig. 5a shows the conversion levels for both 1-pentene and oxygen. Of significance here was that the conversion over alkali promoted catalysts was greater than that observed over the unpromoted V_2O_5. The Li promoted catalyst showed the highest activity for 1-pentene conversion. Also, the trend of increasing ratio of oxygen conver-

sion to C_5 conversion with alkali promotion was not seen in the case of 1-pentene reaction. The formation rates of carbon oxides (Fig. 5b) were also higher over the promoted catalysts, with Li-promoted catalysts giving the highest yield.

Fig. 6 shows the observed formation rates for isomerization and partial oxidation products in 1-pentene oxidation for each catalyst. In general, the alkali promoted catalysts gave higher yields of partial oxidation products, and the largest yields were observed over the K-promoted V_2O_5. This better performance of the potassium-promoted catalyst was even more pronounced for the maleic and phthalic anhydride yields. Notable amounts of a product identified as 3-methyl-2,5-furandione was also detected. The formation rate of maleic and phthalic anhydride was two orders of magnitude higher than that observed when n-pentane was used. 2-pentene and 1,3-pentadiene were also observed at significant levels in the product stream.

It was observed that over the course of the reaction the catalyst changed color from orange–brown to coal black. Post-reaction X-ray diffraction was performed in order to determine if the color change was due to coking or bulk reduction of the V_2O_5. X-ray diffraction data

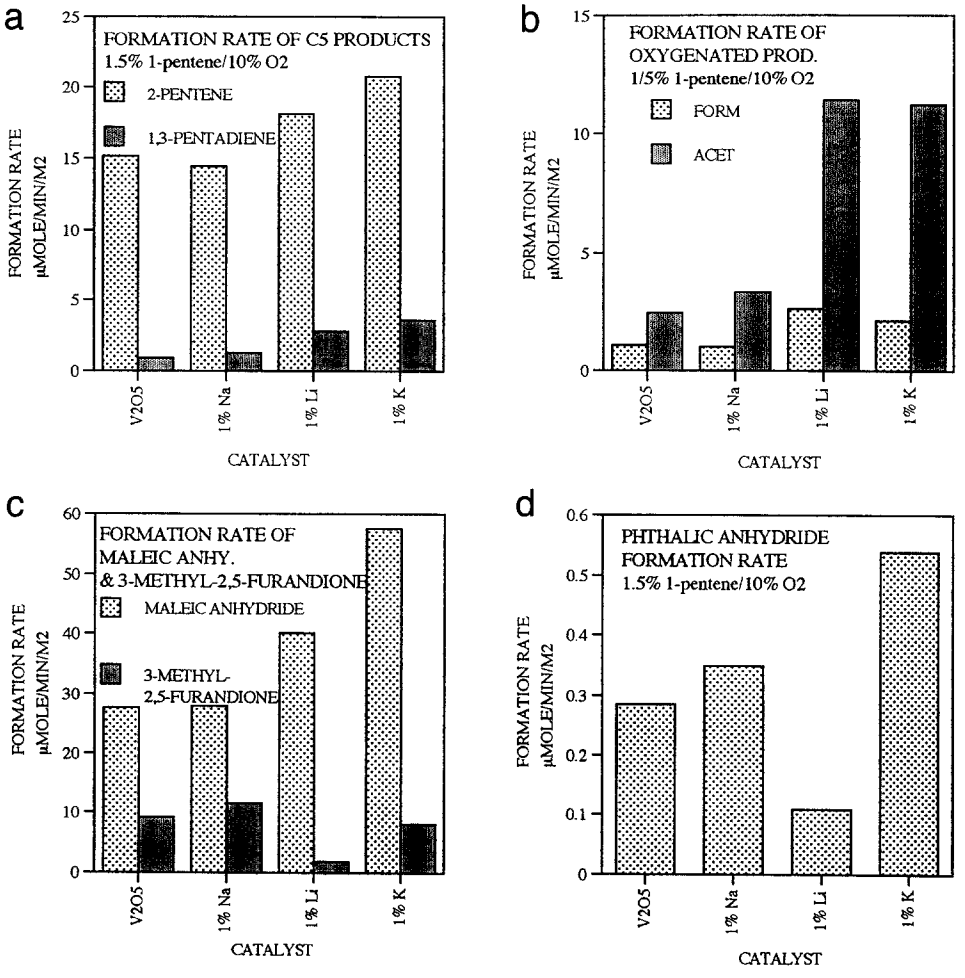

Fig. 6. Formation rates of partial oxidation and isomerization products in 1-pentene oxidation (1.5% 1-pentene, 10% O_2).

indicated that the samples removed from the reactor were made up of a mixture of V_2O_5 and VO_2.

3.3. Temperature-programmed desorption studies

Temperature-programmed desorption studies were performed using n-pentane and 1-pentene as adsorbates in two different sets of experiments. The desorption profiles for each species were obtained by tracing corresponding *m/e*

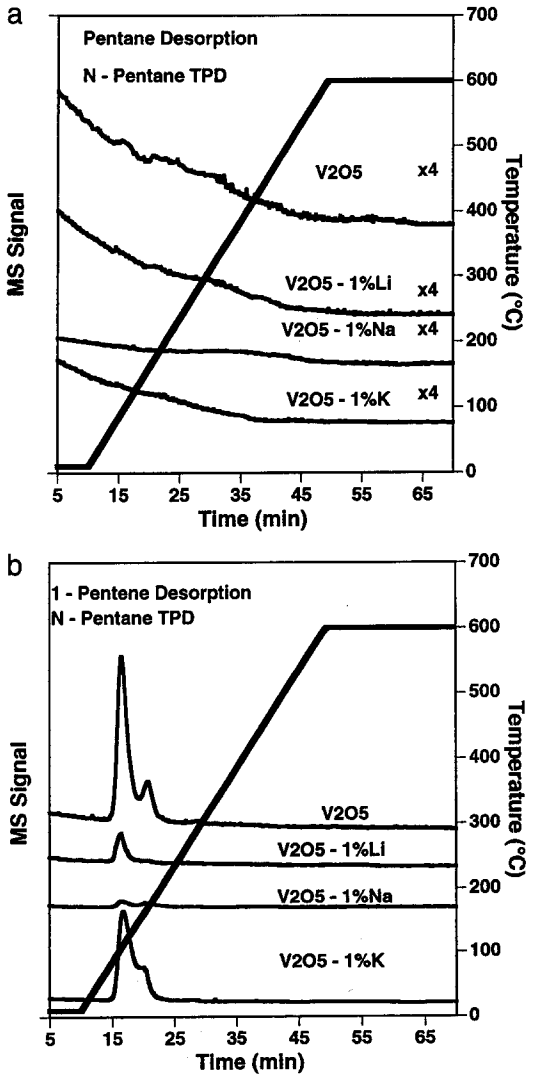

Fig. 7. Desorption profiles of n-pentane and 1-pentene in n-pentane TPD

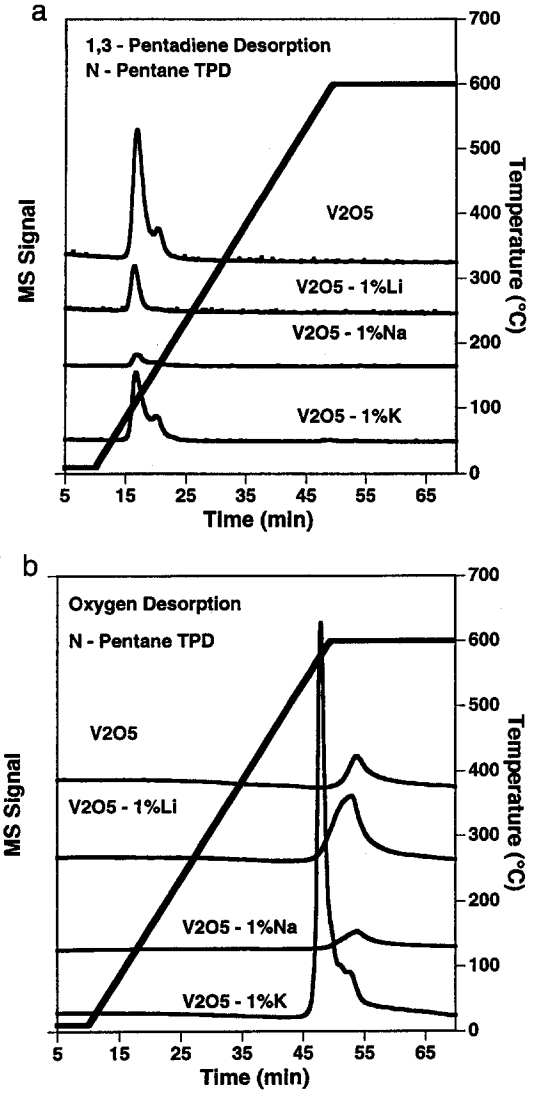

Fig. 8. Desorption profiles of 1,3-pentadiene and oxygen in n-pentane TPD.

signals as follows: n-pentane: 72; 1-pentene: 55, 1,3-pentadiene: 67, oxygen: 32, CO_2: 44, CO: 28, maleic anhydride: 26, 54, 98, phthalic anhydride: 148, 104, 76, 50, acetaldehyde: 27, 29, 30, 43, acetone: 58, formaldehyde: 29, 30, 2-methyl-butane: 43.

Fig. 7 shows the temperature-programmed desorption profiles for n-pentane (7a) and 1-pentene (7b) resulting from n-pentane adsorption. The n-pentane desorption signal was low in all cases, with V_2O_5 and $Li–V_2O_5$ showing

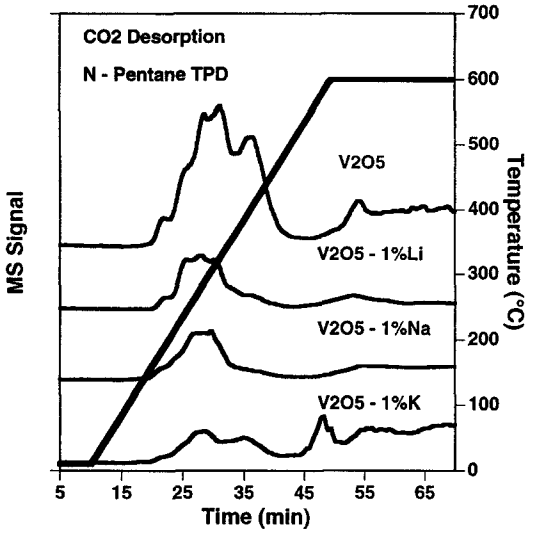

Fig. 9. Desorption profile of CO_2 in n-pentane TPD.

two very small features superimposed over a decreasing background signal at temperatures lower than 100°C. The desorption profile of 1-pentene shows a very strong desorption feature for V_2O_5 while the alkali-promoted catalysts have considerably weaker signals. A similar trend is observed for 1,3-pentadiene desorption profile (Fig. 8a) with V_2O_5 showing the strongest desorption feature and alkali-promoted V_2O_5 showing weaker signals. Also presented in Fig. 8 is the oxygen desorption profiles from all four catalysts. While the oxygen desorption profile of V_2O_5 is characterized by a very small desorption feature that appears several minutes after the catalyst is taken to 600°C, K–V_2O_5 shows a major desorption feature followed by a shoulder peak, the major one appearing at a temperature well below 600°C. Fig. 9 shows the desorption profile for CO_2. For all catalysts CO_2 showed multiple desorption peaks, usually occurring in groups of two. The largest CO_2 desorption was observed from the unpromoted catalyst while the smallest CO_2 signal was seen eluting from K–V_2O_5. Maleic anhydride was observed only on K–V_2O_5, giving a very weak signal. Signals observed over the other catalysts when the m/e ratios of 26 and 54 were monitored could not be verified by m/e ratio of 98 and therefore not reported. There was no phthalic anhydride or appreciable water desorption on any of the catalysts. Other desorption products observed following pentane adsorption included CO, 2-methyl-butane, formaldehyde, acetone and acetaldehyde.

Similar experiments were performed using 1-pentene as the adsorbate. The desorption profiles for major species are presented in Figs. 10–12. As seen in Fig. 10a, once the alkane was replaced by the alkene, the reversible adsorption behavior of the four catalysts became quite similar to one another. Also, it should be noted that the pentene desorption profiles following

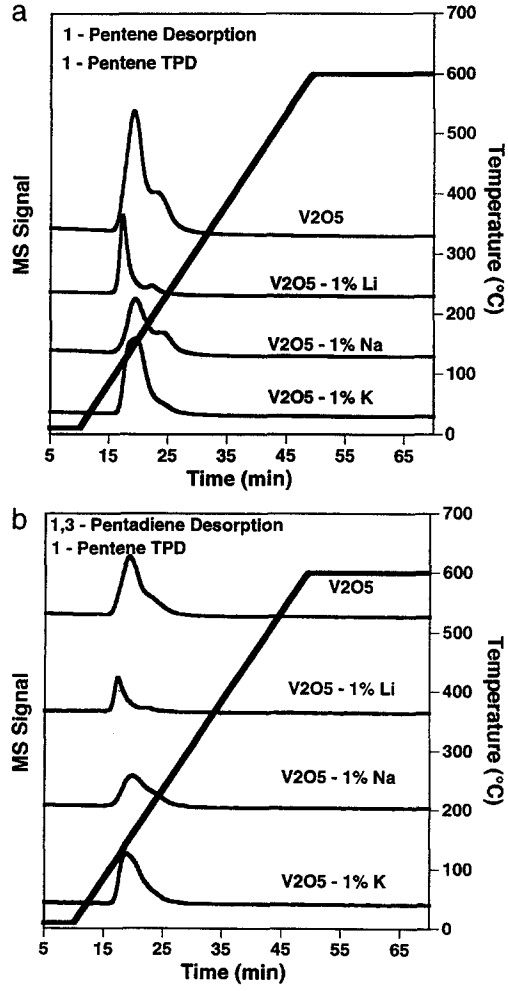

Fig. 10. Desorption profiles of 1-pentene and 1,3-pentadiene in 1-pentene TPD.

pentene and pentane adsorption have very similar shapes except for a small shift to higher temperatures after pentene adsorption. Similarly, the intensity and the temperature maxima for 1,3-pentadiene over the four catalysts did not exhibit any major differences (Fig. 10b). Fig. 11 shows the desorption profiles for oxygen. There is very small oxygen desorption observed from the catalysts except for $K–V_2O_5$ which shows a strong desorption peak just below 600°C, very similar to what was observed following pentane adsorption. Fig. 11b shows maleic anhydride desorption profiles, with desorption maxima taking place at around the same

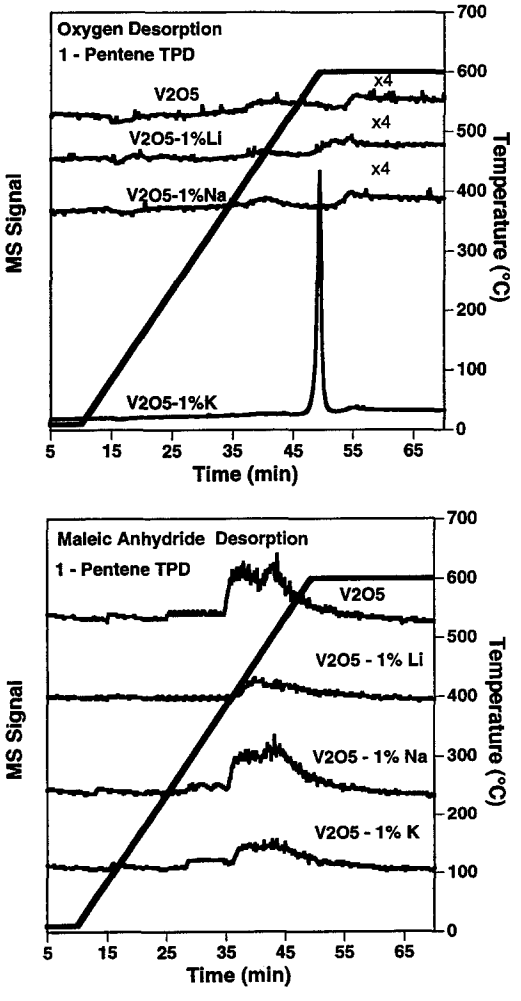

Fig. 11. Desorption profiles of oxygen and maleic anhydride in 1-pentene TPD.

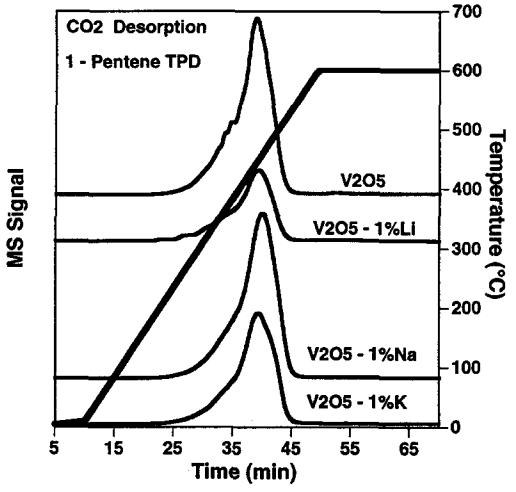

Fig. 12. Desorption profile of CO_2 in 1-pentene TPD.

temperature of 400°C. Fig. 12 shows the CO_2 desorption profiles where V_2O_5 is seen to give the strongest desorption peak.

4. Discussion

The reaction of n-pentane with oxygen over vanadia catalysts was seen to produce CO_2, CO, H_2O, maleic anhydride, phthalic anhydride, and small amounts of 3-methyl-2,5-furandione. At all temperatures investigated, the majority of the products obtained were carbon oxides. An interesting point to consider here is the low amount of intermediate products detected.

Trifiró [8] has suggested that in the partial oxidation of pentane to maleic anhydride over VPO, the reaction intermediates are not allowed to readily desorb. One can argue that the same is true for the reaction of pentane over V_2O_5 with the intermediates being so strongly adsorbed that only the final product, and possibly trace amounts of intermediates are allowed to desorb. In light of the amount of intermediate products observed during 1-pentene studies, however, it is more likely that the high activation barrier of n-pentane necessitates such harsh reaction conditions that intermediates do not survive long enough to be detected.

The detection of small amounts of 3-methyl-2,5-furandione in this study suggests that it may be an intermediate in the production of maleic anhydride over V_2O_5, which occurs via a mechanism slightly different than the one proposed by Centi and Trifiró [9] for anhydride production over $(VO)_2P_2O_7$. Possibly, the last step in the formation of maleic anhydride is the loss and further complete oxidation of the methyl group from 3-methyl-2,5-furandione. The lack of methane in the product stream suggests that the lost methyl group is completely oxidized rather than being released as methane.

TPD studies using pentane as adsorbate have uncovered some interesting trends. Of significance is the fact that the desorption profiles for n-pentane exhibit very few features, indicating very little reversible adsorption. The desorption profiles for dehydrogenation products such as pentene and 1,3-pentadiene seem to be related to catalytic activity, with V_2O_5, which has the highest activity, giving the strongest desorption signal for both pentene and pentadiene. The intensity of the CO_2 peak also seems to be an indicator of the activity of a catalyst since the unpromoted catalyst showed the largest CO_2 desorption peak and the K promoted catalyst showed the smallest. Also the onset of the CO_2 desorption took place at a lower temperature over V_2O_5 than any of the other catalysts. Another important feature of the TPD profiles was seen in oxygen desorption. The largest desorption signal for oxygen was seen over the K promoted catalyst. Also, the oxygen desorption temperature over the K promoted catalyst was at a lower temperature than those seen over the other catalysts. The fact that the $K–V_2O_5$ catalyst was the least active in pentane oxidation, but the most selective in 1-pentene oxidation suggest that the oxygen desorption may signify the loss of some highly active surface oxygen species, which may be essential for the activation of the alkane molecule, but may also be responsible for the further oxidation of the intermediates. Following pentane adsorption, the m/e values of 26, 54, and 98 were monitored in an effort to detect the presence of maleic anhydride. There was a very weak signal observed over the $K–V_2O_5$ catalyst, which was seen in m/e ratios of both 26 and 54. However, it was difficult to detect the same maximum following $m/e = 98$.

When similar experiments were repeated using 1-pentene as the adsorbate, the pentene and pentadiene desorption signals exhibited similar patterns as the ones seen following pentane adsorption. Although the shapes of the patterns were similar, there seemed to be a shift towards higher temperatures following pentene adsorption, which can possibly be explained by a difference in the adsorption geometries of pentane and pentene on the oxide surface. CO_2 desorption profiles following pentene adsorption showed the same trends as those observed following pentane adsorption. Oxygen desorption profiles following pentene adsorption were also very similar to those observed after pentane adsorption, with $K–V_2O_5$ giving a very strong signal and the other catalysts giving almost negligible signals at considerably higher temperatures. The fact that the oxygen desorption takes place at the same temperature following both pentane and pentene adsorption, suggests that these oxygen species are independent of the adsorbate used. The lower intensities observed following pentene adsorption can be explained in terms of the larger oxygen consumption resulting when a more reactive molecule is used as the adsorbate. Maleic anhydride was observed desorbing from all catalysts in small quantities, with the onset of the desorption peak around 400°C. Unlike the case following pentane adsorption, the maleic anhydride profiles were reproduced using all three m/e values, 26, 54, and 98.

It has been suggested in our earlier work [17–19] that the presence of alkali promoters, most notably K, can facilitate the removal of adsorbed surface oxygen species that may play a role in the activation and further complete oxidation of the alkane molecule. It is possible that role of the alkali promoters in the activation

of n-pentane is to facilitate the loss of absorbed surface oxygen species which are important in the activation of n-pentane and possibly the production of complete oxidation products.

When the first hydrogen abstraction step is bypassed by using 1-pentene as the starting molecule, the K-promoted catalyst is seen to have the highest selectivity for both maleic and phthalic anhydrides among all catalysts. This shows that requisite sites necessary for ring closure and template addition steps needed for maleic anhydride and phthalic anhydride readily exist over the vanadia surfaces and the presence of alkali promoters, especially potassium, inhibits the complete oxidation of intermediates and the final products, possibly by eliminating the highly active surface oxygen species or by neutralizing the strong acidic sites on the surface. The formation rate of CO_2 over the unpromoted catalyst was consistently higher than that observed over the promoted catalysts, supporting the above hypothesis.

Another explanation that could partially account for the observed differences in the catalytic behavior of these materials can be found in the X-ray diffraction data, which showed that the intensity ratios from (101) reflections to (010) reflections were higher in the alkali-promoted catalysts. Since V=O double bond sites are predominantly located on the (010) planes of V_2O_5 crystals [20], the higher activity of unpromoted catalysts can be explained by the higher abundance of the V=O sites available on their surfaces.

Over all four catalysts, the formation rate of maleic anhydride was seen to increase as temperature increased. The observed rate for phthalic anhydride, on the other hand, went through a maximum with increasing temperature. These observations seem to be in agreement with the findings reported earlier by Gleaves and Centi [13], who have shown that the desorption rate of phthalic anhydride is slower than that for maleic anhydride and that a maximum in the phthalic anhydride production is seen at temperatures lower than that for maleic anhydride production because at higher temperatures phthalic anhydride is further oxidized to CO_x before it can desorb. Also observed in our studies was the fact that the production of formaldehyde went through a maximum with increasing temperature similar to the one seen for phthalic anhydride, which seems to suggest that formaldehyde and phthalic anhydride are formed by the same reaction pathway, possibly formaldehyde being a side product in the formation of phthalic anhydride.

One important finding in the 1-pentene oxidation experiments is that the catalyst is in a partially reduced form at steady state conditions, as demonstrated by the post-reaction characterization. It was found that in 1-pentene oxidation, it took 24 to 48 h from the time the reactor was put on line until the system reached steady state, as opposed to the 4 to 6 h needed to reach steady state when n-pentane was used as feed. X-ray diffraction experiments done on post-reaction catalyst showed the samples to be a mixture of V_2O_5 and VO_2. It should be noted here that the oxygen in the gas phase was not depleted during these reactions so the catalyst was not reduced as a result of a lack of gas phase oxygen. The formation rate of maleic and phthalic anhydride was approximately two orders of magnitude higher than when n-pentane was used. Also, significant quantities of 3-methyl-2,5-furandione, formaldehyde, and acetaldehyde were produced.

Pentane and pentene oxidation studies as well as post-reaction characterization experiments are in progress using catalysts that are pretreated through a controlled reduction step.

Acknowledgements

Financial support provided for this work by the National Science Foundation through the Grant CTS-9412544 is gratefully acknowledged.

References

[1] N.S. Butt and A. Fish, J. Catal. 5 (1966) 205.
[2] N.S. Butt and A. Fish, J. Catal. 5 (1966) 494.
[3] N.S. Butt and A. Fish, J. Catal. 5 (1966) 508.
[4] G. Centi, J.L. Nieto, and C. Iapalucci, Appl. Catal. 46 (1989) 197.
[5] K.E. Birkeland, W.D. Harding, L. Owend and H.H. Kung, In: eds. S.A. Bradley and J. Stencel, Chem. Characterization Supported Metal Catal. 38 (1993) 880.
[6] C. Fumagalli, G. Golinelli, G. Mazzoni, M. Messori, G. Stefani and F. Trifiró, In: eds. V. C. Corberán and S.V. Bellón, New Developments in Selective Oxidation (Elsevier, Amsterdam, 1994) p. 221.
[7] G. Centi, J.T. Gleaves, G. Golinelli and F. Trifiró, In: eds. B. Delmon and P. Ruiz, New Developments in Selective Oxidation (Elsevier, Amsterdam, 1992) p. 231.
[8] F. Trifiró, Catal. Today 16 (1993) 91.
[9] G. Centi and F. Trifiró, Chem. Eng. Sci. 45 (8) (1990) 2589.
[10] G. Centi, M. Burattini, and F. Trifiró, Appl. Catal. 32 (1987) 353.
[11] G. Busca and G. Centi, J. Am. Chem. Soc. 111 (1989) 46.
[12] G. Centi, J.L. Nieto, D. Pinelli, F. Trifiró and F. Ungarelli, In: eds. G. Centi and F. Trifiró, New Developments in Selective Oxidation (Elsevier, Amsterdam, 1990) p. 635.
[13] J.T. Gleaves and G. Centi, Catal. Today 16 (1993) 69.
[14] G. Golinelli and J.T. Gleaves, J. Mol. Catal. 73 (1992) 353.
[15] G. Centi, J.T. Gleaves, G. Golinelli, S. Perathoner and F. Trifiró, In: eds. C.H. Bartholomew, and J.B. Butt, Catalyst Deactivation (Elsevier, Amsterdam, 1991) p. 449.
[16] U.S. Ozkan, Y. Cai, M.W. Kumthekar and L. Zhang, J. Catal. 142 (1993) 182.
[17] S.A. Driscoll and U.S. Ozkan, J. Phys. Chem. 97 (1993) 11524.
[18] S.A. Driscoll, D.K. Gardner and U.S. Ozkan, Catal. Lett. 25 (1994) 191.
[19] S.A. Driscoll, D.K. Gardner and U.S. Ozkan, J. Catal. 17 (1994) 379.
[20] U.S. Ozkan, Y. Cai and M.W. Kumthekar, Appl. Catal. 96 (1993) 365.